Journal of Materials Chemistry A

PAPER

View Article Online
View Journal | View Issue

Cite this: J. Mater. Chem. A, 2014, 2, 3169

Thermoelectric alloys between PbSe and PbS with effective thermal conductivity reduction and high figure of merit

Heng Wang,*[a] Jianli Wang,[b] Xianlong Cao[c] and G. Jeffrey Snyder*[a]

Received 28th November 2013
Accepted 24th December 2013

DOI: 10.1039/c3ta14929c

www.rsc.org/MaterialsA

The n-type alloys between PbSe and PbS are studied. The effect of alloy composition on transport properties is evaluated and the results are interpreted with theories based on random atomic site substitution. The alloying in $PbSe_{1-x}S_x$ brings thermal conductivity reduction, carrier mobility reduction as well as change of effective mass. When all these factors are evaluated, both experimentally and theoretically, the optimized thermoelectric performance is found to change gradually with alloy composition. High zT can be found in all $PbSe_{1-x}S_x$ alloys. The possibility of achieving significant improvement of zT through alloying is also discussed.

Introduction

Highly efficient thermoelectric materials are essential for waste energy recovery[1] and the development of such materials characterized by high figure of merit zT, defined as $zT = S^2\sigma T/(\kappa_e+\kappa_L)$ (S is the Seebeck coefficient, σ is the electric conductivity, and κ_e and κ_L are the electron and lattice thermal conductivity, respectively), has been the focus of thermoelectric research.[2–5] Alloying is one of the few proven strategies that lead to the best zTs in materials for high temperature applications. Among them are the well known SiGe[6–8] and TAGS[9–12] alloys used in the radioisotope thermoelectric generators (RTGs) powering multiple spacecrafts for decades. Alloying in thermoelectrics provides a wide control of different material properties, including thermal conductivity,[13–15] the band structure,[16–20] mechanical properties[21] and even carrier density:[22,23] all closely related to the thermoelectric performance and zT.

Lead chalcogenides is a family of compounds with promising zT at high temperatures.[24–26] For PbTe, improved zT has been observed in different alloys such as $PbTe_{1-x}Se_x$,[27,28] $Pb_{1-x}Mg_xTe$ (ref. 29) and $Pb_{1-x}Cd_xTe$ (ref. 30). High zT was also found by different studies in PbTe–MTe[31–34] (M: Ca, Mg, Sr, Ba) and PbTe–CdTe,[35,36] where they were shown to have nano-scale features that are also suggested as important for good thermoelectric properties. For the less studied chalcogenides, high zT was also reported for systems such as PbSe–PbS,[37] PbSe–MSe[38–40] (M: Ca, Sr, Ba), and PbS–XS[41,42] (X: Ca, Sr, Zn, Cd), where similar nanostructures were also observed.

The old concept of solid solutions based on random atomic site substitution is however far from obsolete. Transport properties of many high zT materials from recent studies[27,43–45] have followed theories based on this concept. By studying a specific case of n-type $PbTe_{1-x}Se_x$, simple criteria[46] were concluded for beneficial disorder when there is no change in the band structure.

Like $PbTe_{1-x}Se_x$, PbSe and PbS also form complete solid solutions, according to the phase diagram. A previous study[37] on PbS added to PbSe focused on the nano scale features induced by the small amount of PbS addition whereas a study of the entire composition range especially on the PbS rich side is still missing. Recently we have studied[47] stoichiometric $PbSe_{1-x}S_x$, where the dependence of mobility and lattice thermal conductivity on alloy composition suggested zT improvement in the alloys. In this report we present a comprehensive study of $PbSe_{1-x}S_x$ with different doping levels (by Cl substitution of the anion) and quantitative analysis based on the random solid solution model. The transport properties are well explained with this simple picture with a minimal number of fitting parameters and the previously observed nano-scale feature in this system does not produce further lattice thermal conductivity reduction. With important material parameters determined for this alloy system the effect of disorder on thermoelectric performance was evaluated using the quality factor. We demonstrate that high zT can be found for any composition of $PbSe_{1-x}S_x$, while more significant improvement will need additional material engineering.

Results and discussion

All samples are single phase when examined with X-ray diffraction (Fig. 1a). The lattice constant decreases with

[a]Materials Science, California Institute of Technology, Pasadena, CA 91125, USA. E-mail: hengwang@caltech.edu; jsnyder@caltech.edu

[b]Jiangsu Key Laboratory for Design and Manufacture of Micro/Nano Biomedical Instruments, Department of Mechanical Engineering, Southeast University, Nanjing 210096, China

[c]Department of Metallurgy and Materials Engineering, Chongqing University of Science and Technology, Chongqing 401331, China

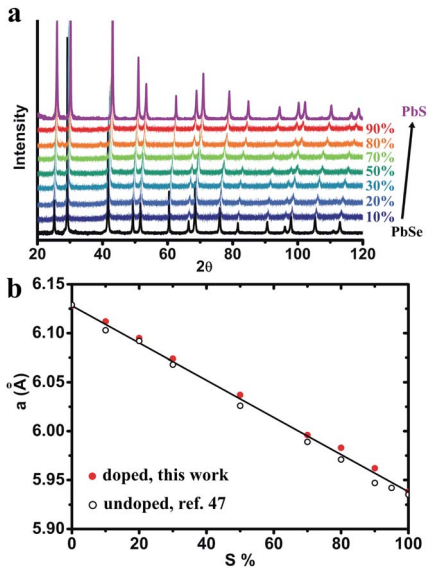

Fig. 1 The (a) XRD patterns and (b) lattice constants of $PbSe_{1-x}S_x$ samples, following Vegard's law expected for solid solutions.

increasing S content following Vegard's law, consistent with the results on undoped samples[47] (Fig. 1b). Polished surfaces showed a homogeneous morphology (Fig. 2) under SEM where S and Se are found evenly distributed throughout the matrix and no precipitates with enough compositional contrast down to 50 nm can be seen. These are behaviors of solid solutions with statistically random atomic distribution. Recently many lead chalcogenides[31–33,35,36,39,48–51] (including PbSe with PbS addition < 16%) are found with nanostructures on the <10 nm scale using TEM. These features on the nanoscale are not necessarily in conflict with our SEM observation at larger scales. We thus refer to the $PbSe_{1-x}S_x$ system as "alloys", which includes the case of random solid solutions as well as mixtures with multiple phases.

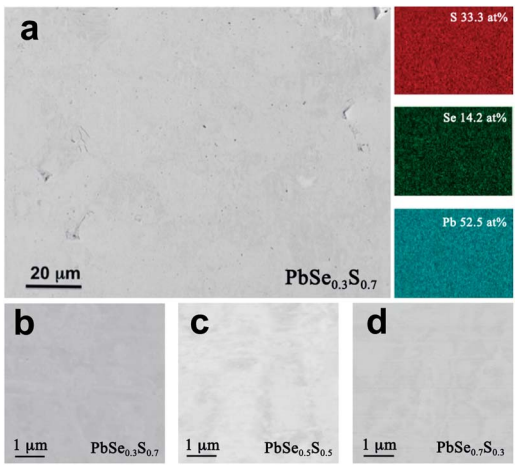

Fig. 2 The back scattered SEM images of $PbSe_{1-x}S_x$, 3 compositions are shown as examples: (a) and (b) $PbSe_{0.3}S_{0.7}$, (c) $PbSe_{0.5}S_{0.5}$, and (d) $PbSe_{0.7}S_{0.3}$. EDS mapping from (a) is also shown and no phase segregation or precipitates down to 50 nm can be found.

Fig. 3a shows the Seebeck coefficient as a function of Hall carrier density (the Pisarenko relation) for some different alloy compositions. The (density-of-state, DOS) effective masses (m_d^*) are estimated under the assumption of a single Kane band (SKB) model[52] with combined carrier scattering of acoustic phonon scattering as well as polar scattering from optical phonons[53] and alloy scattering[46] (detailed equations for calculation can be found in ref. 53). The $PbSe_{1-x}S_x$ alloys have different m_d^* values depending on the value of x, which can be explained by the different effective masses of the conduction band for binary PbSe[54] (0.27 m_e) and PbS[53] (0.39 m_e). As shown in the inset of Fig. 3a, the effective mass increases with increasing S content, roughly following the linear extrapolation between two binary compounds (solid lines are calculated for each composition with m_d^* from this trend). An abrupt change of DOS effective mass, which is often an indication of band convergence[19,55] is not observed. Within experimental uncertainty the effective mass changes linearly, although there could be slight bowing (nonlinearity) as seen in some III–V semiconductor alloys.[56] For dilute alloys the difference in effective mass is

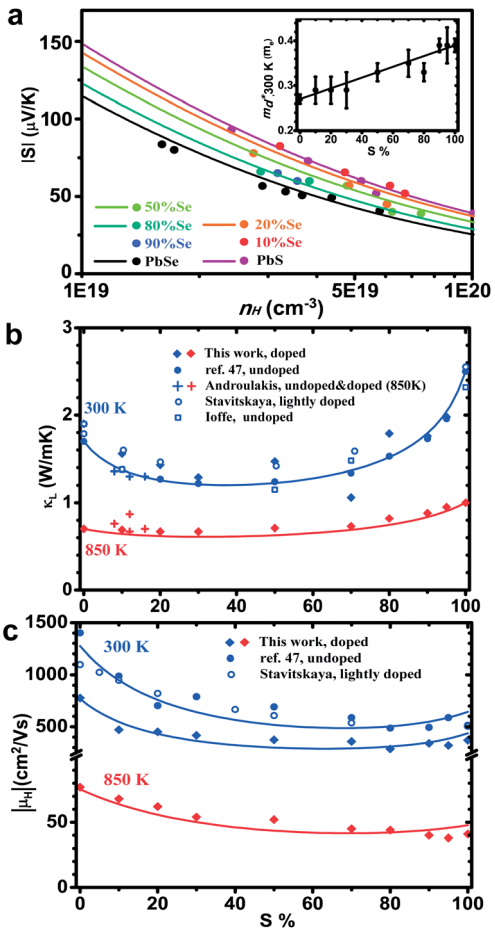

Fig. 3 The influence of alloy composition on transport properties: (a) Seebeck *versus* carrier density for different compositions, the inset shows the DOS effective mass m_d^*, uncertainties are estimated based on the number of samples studied. (b) Lattice thermal conductivity and (c) Hall mobility reduction at both 300 K and 850 K.

comparable with experimental uncertainty, which is probably why no difference in effective mass was observed in ref. 37.

Besides having influence on effective mass the random substitution also introduces lattice thermal conductivity reduction as well as mobility reduction, as discussed previously in the n-type $PbTe_{1-x}Se_x$ system.[46] Fig. 3b shows the lattice thermal conductivity κ_L at both 300 K and 850 K for alloys with different sulfur contents. The 300 K data include κ_L calculated from doped samples (the diamonds) and undoped ones[47] (solid circles) in which κ_L dominates the measured total thermal conductivity κ. The open circles are results reported by Stavitskaya[57] for undoped/lightly doped samples and the open squares are results reported by Ioffe.[15] For 850 K only the calculated κ_L values from doped samples are shown due to the bipolar conduction in undoped samples. For such calculation the Lorenz number L was calculated from the reduced chemical potentials (derived from Seebeck coefficients) under the SKB model with combined scattering mechanisms. For the optimum doped samples L decreases from 2.0 at 300 K to 1.4 at 850 K, with 5% variance among samples. Detailed equations are described in ref. 53.

At both temperatures the experimental results follow closely the calculated κ_L (solid curve) for disordered solid solutions. The calculation is based on the Klemens' model[58,59] that links the lattice thermal conductivity of alloys with a perfect system without disorder. At high temperature if the dominant scattering mechanisms for phonons are Umklapp scattering and point defect scattering, then:

$$\frac{\kappa_{L,\mathrm{alloy}}}{\kappa_{L,\mathrm{pure}}} = \frac{\arctan(u)}{u}, u^2 = \frac{\pi\theta_D\Omega}{2\hbar v^2}\kappa_{L,\mathrm{pure}}\Gamma \quad (1)$$

$\kappa_{L,\mathrm{alloy}}$ and $\kappa_{L,\mathrm{pure}}$ are the lattice thermal conductivities of the alloy and the perfect (virtual) crystal without disorder, respectively. v is the average speed of sound, θ_D is the Debye temperature, and Ω is the volume per atom. The scattering parameter Γ includes influence from mass difference, bonding force difference and strain field induced by point defects for binary ($A_{1-x}B_x$ type) or pseudo-binary ($AB_{1-x}C_x$ type) systems:[13,60]

$$\Gamma = x(1-x)\left[\left(\frac{\Delta M}{M}\right)^2 + \varepsilon\left(\frac{a-a_{\mathrm{pure}}}{x a_{\mathrm{pure}}}\right)^2\right] \quad (2)$$

ΔM and $\Delta\alpha$ are the differences in mass and lattice constants between the two binary compounds; M and α are the molar mass and lattice constant of the virtual crystal. The parameter ε is related to the elastic properties and is generally treated as a fitting parameter.[13,61] Nonetheless the value of ε could be estimated using:[13,58,62]

$$\varepsilon = \frac{2}{9}\left[(G+6.4\gamma)\frac{1+r}{1-r}\right]^2 \quad (3)$$

where γ is the Grüneisen parameter and r is the Poisson ratio. G is a ratio between the relative change of bulk modulus $\Delta K/K$ and the bonding length $\Delta R/R$. The ratio G is relatively constant within similar material systems,[63,64] for example for covalent IV and III–V structures $G = 4$, for more ionic II–VI and I–VII structures $G = 3$ and for complex oxide structures $G = 9$. For lead chalcogenides $G = 3$ and ε calculated for PbSe and PbS is 110 and 150, respectively. All properties of the virtual crystal are taken as the linear average of two binary compounds, which are listed in ref. 53. There are no fitting parameters involved in the calculation of κ_L for the alloys between PbSe and PbS.

As shown in Fig. 3b the reported[37] κ_L for PbSe with PbS addition ($\leq$16%), including those where nanostructures are observed, exhibit the same magnitude of reduction compared with results from this study both at 300 K and 850 K.

The effect coupled with thermal conductivity reduction in solid solutions is the mobility reduction due to the introduced alloy scattering of carriers,[65–69] the magnitude of which in the case of $PbSe_{1-x}S_x$ at both 300 K and 850 K is shown in Fig. 3c. Both doped and undoped samples[47] are shown for 300 K (together with values reported by Stavitskaya[57]) and only doped samples are shown for 850 K. The observed mobility reduction is not symmetric: it decreases quickly as PbS is added to PbSe whereas only a marginal reduction in mobility is seen when PbSe is introduced to PbS, regardless of doping or temperature.

For both PbS and PbSe at room temperature, both deformation potential scattering (*i.e.* acoustic phonon scattering) and polar scattering from optical phonons are important.[53] The relaxation time for each mechanism can be expressed as:

$$\tau_{\mathrm{ac}} = \frac{\pi\hbar^4 C_l}{2^{1/2}{m_b}^{*3/2}(k_B T)^{3/2}\Xi^2}\left(\varepsilon+\varepsilon^2\alpha\right)^{-1/2}(1+2\varepsilon\alpha)^{-1} \times\left[1-\frac{8\alpha(\varepsilon+\varepsilon^2\alpha)}{3(1+2\varepsilon\alpha)^2}\right]^{-1} \quad (4)$$

$$\tau_{\mathrm{po}} = \frac{4\pi\hbar^2\varepsilon^{1/2}}{2^{1/2}(k_B T)^{1/2}e^2{m_b}^{*1/2}\left({\varepsilon_\infty}^{-1}-{\varepsilon_0}^{-1}\right)}(1+2\varepsilon\alpha)^{-1}(1+\varepsilon\alpha)^{1/2} \times\left\{\left[1-\delta\ ln\left(1+\frac{1}{\delta}\right)\right]-\frac{2\alpha\varepsilon(1+\varepsilon\alpha)}{(1+2\varepsilon\alpha)^2} \times\left[1-2\delta+2\delta^2\ ln\left(1+\frac{1}{\delta}\right)\right]\right\}^{-1} \quad (5)$$

$$\delta(\varepsilon) = \frac{e^2{m_d}^{*1/2}N_V^{2/3}}{2^{1/2}\varepsilon(k_B T)^{1/2}\pi\hbar\varepsilon_\infty}(1+\varepsilon\alpha)^{-10}L_1^{1/2} \quad (6)$$

where m_d^* is the total DOS effective mass. C_l is the average longitudinal elastic constant.[70] N_v is the degeneracy of the conduction band. Ξ is the deformation potential coefficient. ε_0 and ε_∞ are the static and high frequency dielectric constants, respectively. ε is the reduced carrier energy E/k_BT and $\alpha = k_BT/E_g$, where E_g is the gap between two interacting bands at the L point of the Brillouin zone. These properties of alloys are also taken as the linear average of two binary compounds. The generalized Fermi integral ${}^nL_l^m$ is defined by:

$${}^nL_l^m = \int_0^\infty\left(-\frac{\partial f}{\partial\varepsilon}\right)\varepsilon^n\left(\varepsilon+\varepsilon^2\alpha\right)^m(1+2\varepsilon\alpha)^l d\varepsilon \quad (7)$$

In alloys a new scattering mechanism is introduced due to the atomic substitution. Relaxation time of this alloy scattering in narrow gap semiconductors can be written as:[46,71,72]

$$\tau_{\text{alloy}} = \frac{8\hbar^4}{3\sqrt{2}\pi\Omega x(1-x)U^2 {m_b}^{*3/2}(k_B T)^{1/2}}(\varepsilon+\varepsilon^2\alpha)^{-1/2}(1+2\varepsilon\alpha)^{-1} \times\left[1-\frac{8\alpha(\varepsilon+\varepsilon^2\alpha)}{3(1+2\varepsilon\alpha)^2}\right]^{-1} \quad (8)$$

Ω is the volume per atom. x is the percentage of substituted atoms. U is the alloy scattering potential, which is generally believed to be the energy offset of atomic levels that forms the conduction/valence band. Such a view cannot entirely explain why U is found[46] to be around 1 eV for n-type $PbTe_{1-x}Se_x$ while the conduction band offset[73] between PbTe and PbSe is only 0.1 eV. In this study, U is taken as the only fitting parameter and $U = 1$ eV is determined. The similar U value is consistent with the similar conduction band offset, which is[73] 0.15 eV between PbSe and PbS.

The solid lines in Fig. 3c show the calculated mobilities assuming a constant $\eta = E_F/k_B T$ of −0.3 (for undoped), 3.6 (for doped) and −0.2 (for doped samples at 850 K). The calculation, based on the classic concept of solid solutions, matches the observed results reasonably well in all cases. The asymmetrical mobility reduction is also reproduced by the calculation. The alloy scattering potential U is constant throughout the composition range, which means the asymmetry is not due to the different magnitude of scattering from S and Se. Actually, as shown by the Pisarenko relation, m_d^* changes (through change of m_b^*) with the alloy composition which is responsible for the asymmetrical mobility reduction.

Fig. 4a shows the zT value of the alloys at different temperatures. The carrier densities of samples shown are carefully controlled: $n_{H,300\ K} = 3 \times 10^{19}$ cm^{-3} (±10%) for alloys with $x < 0.5$ and 5×10^{19} cm^{-3} (±10%) for alloys with $x \geq 0.5$. The Seebeck coefficient values at 850 K for these samples are about the same at −190 μV K^{-1} (±10%). These will lead to zT values close to the optimized ones at 850 K for all compositions. At 850 K, zT is found to increase when substituting S in PbS with Se, while it is found to decrease when substituting Se in PbSe with S. Neither of these changes, however, is significant especially when compared with the averaged zT from the rule of mixing between PbSe and PbS (the dashed lines).

A simple estimate[46] of whether a disorder is thermoelectrically beneficial or not can be done by evaluating:

$$\left.\frac{d}{dx}\frac{\Delta B}{B_{\text{pure}}}\right|_{x=0} = 7.2\times10^3\frac{\left(\Omega^{1/3}/\text{Å}\right)}{(T/K)} \times\left\{\frac{18.5}{(\theta_D/K)}\left(\kappa_{L,\text{pure},300K}/\text{W m}^{-1}\text{ K}^{-1}\right) \times\left[\left(\frac{\Delta M}{M}\right)^2+\varepsilon\left(\frac{\Delta\alpha}{\alpha}\right)^2\right] -0.038(C_l/\text{GPa})\left(\Omega^{2/3}/\text{Å}^2\right)\left(\frac{U}{\Xi}\right)^2\right\} \quad (9)$$

or

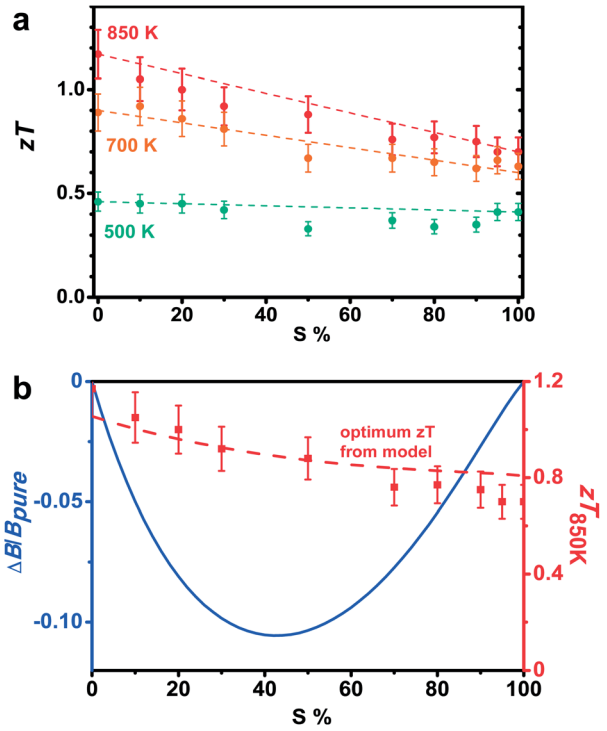

Fig. 4 (a) Measured zT *versus* composition at different temperatures for $PbSe_{1-x}S_x$. The dashed lines are the linear average between zT of the two binary compounds PbSe and PbS. The error bar represents a magnitude of 10% uncertainty on zT. (b) The relative change of quality factor with composition (blue line) and change of zT (red dashed line and squares) at 850 K with composition. The dashed line is the calculated maximum zT for each composition.

$$\left.\frac{d}{dx}\frac{\Delta B}{B_{\text{pure}}}\right|_{x=0} = \frac{\pi K\Omega}{4k_B T}\left\{\frac{1}{4\gamma^2}\left[\left(\frac{\Delta M}{M}\right)^2+\varepsilon\left(\frac{\Delta\alpha}{\alpha}\right)^2\right]-10.6\left(\frac{U}{\Xi}\right)^2\right\} \quad (10)$$

Both (9) and (10), yielded negative values for the system of $PbSe_{1-x}S_x$ for the two limiting cases of PbSe and PbS with a small addition of each other. So a noticeable increase of zT is not expected by theory as well when a solid solution is formed. Fig. 4b shows the relative change of quality factor in solid solutions as a function of composition given by:

$$\frac{\Delta B}{B_{\text{pure}}} = \frac{u/\arctan(u)}{1+\frac{3\pi^2 x(1-x)C_l\Omega}{8k_B T}\left(\frac{U}{\Xi}\right)^2}-1 \quad (11)$$

Eqn (11) reduces to (9) and (10) in the dilute limit. Being consistent with (9) and (10), Fig. 4b indicates that ΔB stays negative throughout the composition range. The calculated optimized zT based on the described models is shown as a dashed line in Fig. 4b, much higher zT over the optimized ones of each binary compound is not very likely.

PbS and PbSe have different optimum values of zT, and the alloys between them have different effective masses depending on the composition. Nonetheless as m_d^* (thus m_I^*) is approximated by a linear extrapolation between the two compounds, so

will the quality factor of the virtual system to which the change in alloys is compared. In general cases when a gradual linear extrapolation is obeyed by all material properties (m_I^*, Ξ, C_l, and N_v) that depend on composition, the criteria (9) and (10) can still be applied to estimate the change of zT relative to the weighed average of optimum zT of the two compounds.

Conclusions

n-type $PbSe_{1-x}S_x$ ($0 \leq x \leq 1$) is studied and the observed transport properties can be well understood assuming random anion site substitution. The mobility shows asymmetrical reduction, which is due to the different effective masses in the alloys. Despite the significant thermal conductivity reduction and high zT over the entire composition range, the alloys between PbSe and PbS do not produce significant increase of zT over those of PbSe and PbS, which agree with the criteria of beneficial disorder for thermoelectrics.

Experimental methods

Samples are prepared by the conventional melting technique, with additional care to achieve homogenization while avoiding treatments that lead to microstructural formation or phase segregation. Elements were loaded into quartz ampoules and sealed under vacuum $<10^{-4}$ torr. The dopant of Cl was added in the form of $PbCl_2$ and S was dehydrated. The ampoules were heated to 650 K in 4 hours and soaked for 2 hours to enable the initial reaction of Pb and S, the temperature was then increased to 1373 K and held for 72 hours followed by quenching and annealing at 900 K for 72 hours. Ingots were ground and pressed using an induction heated hot press[74] under an Ar atmosphere at 823 K for 60 minutes with a 40 MPa load. The obtained disks were 12 mm in diameter, around 1 mm thick with relative densities above 98%. The temperature dependent resistivity and Hall coefficient within the plane were measured by the Van der Pauw method.[75] Cross-plane Seebeck coefficient at different temperatures was measured under oscillating temperatures with Chromel-Nb thermocouples.[76] Thermal conductivity was calculated as $\kappa = dD_TC_p$, with the thermal diffusivity D_T measured along the cross-plane direction by the laser flash method (Netzsch LFA 457) under Argon flow using the Cowan model plus pulse correction. The heat capacity C_p was determined using the equation C_p/k_B atom$^{-1} = 3.07 + 4.7 \times 10^{-4}$ (T/K-300) by fitting high quality measurement results.[77] All properties are isotropic based on a previous study on PbSe. For each measurement data were collected during both heating and cooling and no hysteresis or change in properties were observed. The uncertainty of each measurement is about 5% which when combined could lead to a maximum of 20% uncertainty in the zT value.

Acknowledgements

H. W. and G. J. S. would like to thank AFOSR MURI FA9550-10-1-0533 and NASA/JPL for funding. X. C. thanks the Natural Science Foundation Project of Chongqing CSTC (project no. cstc2011jjA50011) and Research Foundation of Chongqing University of Science & Technology (project no. CK2010Z08) for funding.

Notes and references

1 L. E. Bell, *Science*, 2008, **321**, 1457–1461.
2 X. Shi, J. Yang, J. R. Salvador, M. F. Chi, J. Y. Cho, H. Wang, S. Q. Bai, J. H. Yang, W. Q. Zhang and L. D. Chen, *J. Am. Chem. Soc.*, 2011, **133**, 7837–7846.
3 G. J. Snyder and E. S. Toberer, *Nat. Mater.*, 2008, **7**, 105–114.
4 J. R. Sootsman, D. Y. Chung and M. G. Kanatzidis, *Angew. Chem., Int. Ed. Engl.*, 2009, **48**, 8616–8639.
5 M. Zebarjadi, K. Esfarjani, M. S. Dresselhaus, Z. F. Ren and G. Chen, *Energy Environ. Sci.*, 2012, **5**, 5147–5162.
6 C. B. Vining, *J. Appl. Phys.*, 1991, **69**, 331–341.
7 J. P. Dismukes, L. Ekstrom, E. F. Steigmeier, I. Kudman and D. S. Beers, *J. Appl. Phys.*, 1964, **35**, 2899–2907.
8 D. M. Rowe, V. S. Shukla and N. Savvides, *Nature*, 1981, **290**, 765–766.
9 E. A. Skrabek and D. S. Trimmer, in *CRC Handbook of Thermoelectrics*, ed. D. M. Rowe, CRC Press, Boca Raton, 1995, pp. 267–275.
10 E. M. Levin, S. L. Bud'ko and K. Schmidt-Rohr, *Adv. Funct. Mater.*, 2012, **22**, 2766–2774.
11 Y. Chen, T. J. Zhu, S. H. Yang, S. N. Zhang, W. Miao and X. B. Zhao, *J. Electron. Mater.*, 2010, **39**, 1719–1723.
12 T. Zhu, H. Gao, Y. Chen and X. Zhao, *J. Mater. Chem. A*, DOI: 10.1039/C3TA15147F.
13 B. Abeles, *Phys. Rev.*, 1963, **131**, 1906–1911.
14 C. M. Bhandari and D. M. Rowe, *J. Phys. D: Appl. Phys.*, 1977, **10**, L59–L61.
15 A. V. Ioffe and A. F. Ioffe, *Phys. Solid State*, 1960, **2**, 719–728.
16 P. E. Batson and J. F. Morar, *Appl. Phys. Lett.*, 1991, **59**, 3285–3287.
17 F. Ben Zid, A. Bhouri, H. Mejri, M. Said, N. Bouarissa, J. L. Lazzari, F. A. d'Avitaya and J. Derrien, *Physica B*, 2002, **322**, 225–235.
18 V. K. Zaitsev, M. I. Fedorov, E. A. Gurieva, I. S. Eremin, P. P. Konstantinov, A. Y. Samunin and M. V. Vedernikov, *Phys. Rev. B: Condens. Matter Mater. Phys.*, 2006, **74**, 045207.
19 W. Liu, X. Tan, K. Yin, H. Liu, X. Tang, J. Shi, Q. Zhang and C. Uher, *Phys. Rev. Lett.*, 2012, **108**, 166601.
20 M. S. Park, J.-H. Song, J. E. Medvedeva, M. Kim, I. G. Kim and A. J. Freeman, *Phys. Rev. B: Condens. Matter Mater. Phys.*, 2010, **81**, 155211.
21 F. Ren, E. D. Case, E. J. Timm and H. J. Schock, *Philos. Mag.*, 2007, **87**, 4907–4934.
22 Y. Gelbstein, Z. Dashevsky and M. P. Dariel, *J. Appl. Phys.*, 2008, **104**, 033702.
23 E. S. Toberer, C. A. Cox, S. R. Brown, T. Ikeda, A. F. May, S. M. Kauzlarich and G. J. Snyder, *Adv. Funct. Mater.*, 2008, **18**, 2795–2800.
24 M. G. Kanatzidis, *Chem. Mater.*, 2010, **22**, 648–659.
25 A. D. LaLonde, Y. Z. Pei, H. Wang and G. J. Snyder, *Mater. Today*, 2011, **14**, 526–532.
26 Y. Z. Pei, H. Wang and G. J. Snyder, *Adv. Mater.*, 2012, **24**, 6125–6135.

27 Y. Pei, X. Shi, A. LaLonde, H. Wang, L. Chen and G. J. Snyder, *Nature*, 2011, **473**, 66–69.
28 Q. Zhang, F. Cao, W. Liu, K. Lukas, B. Yu, S. Chen, C. Opeil, D. Broido, G. Chen and Z. Ren, *J. Am. Chem. Soc.*, 2012, **134**, 10031–10038.
29 Y. Z. Pei, A. D. LaLonde, N. A. Heinz, X. Y. Shi, S. Iwanaga, H. Wang, L. D. Chen and G. J. Snyder, *Adv. Mater.*, 2011, **23**, 5674–5678.
30 Y. Pei, A. D. LaLonde, N. A. Heinz and G. J. Snyder, *Adv. Energy Mater.*, 2012, **2**, 670–675.
31 M. Ohta, K. Biswas, S. H. Lo, J. Q. He, D. Y. Chung, V. P. Dravid and M. G. Kanatzidis, *Adv. Energy Mater.*, 2012, **2**, 1117–1123.
32 K. Biswas, J. He, I. D. Blum, C. I. Wu, T. P. Hogan, D. N. Seidman, V. P. Dravid and M. G. Kanatzidis, *Nature*, 2012, **489**, 414–418.
33 K. Biswas, J. Q. He, G. Y. Wang, S. H. Lo, C. Uher, V. P. Dravid and M. G. Kanatzidis, *Energy Environ. Sci.*, 2011, **4**, 4675–4684.
34 L. D. Zhao, H. J. Wu, S. Q. Hao, C. I. Wu, X. Y. Zhou, K. Biswas, J. Q. He, T. P. Hogan, C. Uher, C. Wolverton, V. P. Dravid and M. G. Kanatzidis, *Energy Environ. Sci.*, 2013, **6**, 3346.
35 M. K. Han, X. Y. Zhou, C. Uher, S. J. Kim and M. G. Kanatzidis, *Adv. Energy Mater.*, 2012, **2**, 1218–1225.
36 K. Ahn, M. K. Han, J. Q. He, J. Androulakis, S. Ballikaya, C. Uher, V. P. Dravid and M. G. Kanatzidis, *J. Am. Chem. Soc.*, 2010, **132**, 5227–5235.
37 J. Androulakis, I. Todorov, J. He, D. Y. Chung, V. Dravid and M. Kanatzidis, *J. Am. Chem. Soc.*, 2011, **133**, 10920–10927.
38 H. Wang, Z. M. Gibbs, Y. Takagiwa and G. Snyder, *Energy Environ. Sci.*, 2014, DOI: 10.1039/C3EE43438A.
39 Y. Lee, S.-H. Lo, J. Androulakis, C.-I. Wu, L.-D. Zhao, D.-Y. Chung, T. P. Hogan, V. P. Dravid and M. G. Kanatzidis, *J. Am. Chem. Soc.*, 2013, **135**, 5152–5160.
40 L. D. Zhao, S. Hao, S. H. Lo, C. I. Wu, X. Zhou, Y. Lee, H. Li, K. Biswas, T. P. Hogan, C. Uher, C. Wolverton, V. P. Dravid and M. G. Kanatzidis, *J. Am. Chem. Soc.*, 2013, **135**, 7364–7370.
41 L. D. Zhao, J. He, S. Hao, C. I. Wu, T. P. Hogan, C. Wolverton, V. P. Dravid and M. G. Kanatzidis, *J. Am. Chem. Soc.*, 2012, **134**, 16327–16336.
42 L. D. Zhao, J. He, C. I. Wu, T. P. Hogan, X. Zhou, C. Uher, V. P. Dravid and M. G. Kanatzidis, *J. Am. Chem. Soc.*, 2012, **134**, 7902–7912.
43 X. Liu, T. Zhu, H. Wang, L. Hu, H. Xie, G. Jiang, G. J. Snyder and X. Zhao, *Adv. Energy Mater.*, 2013, **3**, 1238–1244.
44 H. Xie, H. Wang, Y. Pei, C. Fu, X. Liu, G. J. Snyder, X. Zhao and T. Zhu, *Adv. Funct. Mater.*, 2013, **23**, 5123–5130.
45 Z. Zhou, C. Uher, A. Jewell and T. Caillat, *Phys. Rev. B: Condens. Matter Mater. Phys.*, 2005, **71**, 235209.
46 H. Wang, A. D. LaLonde, Y. Z. Pei and G. J. Snyder, *Adv. Funct. Mater.*, 2013, **23**, 1586–1596.
47 J. L. Wang, H. Wang, G. J. Snyder, X. Zhang, Z. H. Ni and Y. F. Chen, *J. Phys. D: Appl. Phys.*, 2013, **46**, 405301.
48 J. Q. He, S. N. Girard, M. G. Kanatzidis and V. P. Dravid, *Adv. Funct. Mater.*, 2010, **20**, 764–772.
49 S. N. Girard, J. Q. He, X. Y. Zhou, D. Shoemaker, C. M. Jaworski, C. Uher, V. P. Dravid, J. P. Heremans and M. G. Kanatzidis, *J. Am. Chem. Soc.*, 2011, **133**, 16588–16597.
50 J. He, J. Androulakis, M. G. Kanatzidis and V. P. Dravid, *Nano Lett.*, 2012, **12**, 343–347.
51 S. Johnsen, J. Q. He, J. Androulakis, V. P. Dravid, I. Todorov, D. Y. Chung and M. G. Kanatzidis, *J. Am. Chem. Soc.*, 2011, **133**, 3460–3470.
52 Y. I. Ravich, B. A. Efimova and I. A. Smirnov, *Semiconducting lead chalcogenides*, Plenum Press, New York, 1970.
53 H. Wang, E. Schechtel, Y. Pei and G. J. Snyder, *Adv. Energy Mater.*, 2013, **3**, 488–495.
54 H. Wang, Y. Pei, A. D. LaLonde and G. J. Snyder, *Proc. Natl. Acad. Sci. U. S. A.*, 2012, **109**, 9705–9709.
55 V. S. Gaidukova, R. S. Erofeev and V. N. Ovechkina, *Inorg. Mater.*, 1981, **17**, 169–172.
56 I. Vurgaftman, J. R. Meyer and L. R. Ram-Mohan, *J. Appl. Phys.*, 2001, **89**, 5815.
57 T. S. Stavitskaya, DSc dissertation, A. F. Ioffe Physical-Technical Institute, 1968.
58 P. G. Klemens, *Proc. Phy. Soc. London Sect A*, 1955, **68**, 1113–1128.
59 P. G. Klemens, *Phys. Rev.*, 1960, **119**, 507–509.
60 V. K. Zaitsev, E. N. Tkalenko and E. N. Nikitin, *Sov. Phy. Solid State*, 1969, **11**, 221–224.
61 G. T. Alekseeva, B. A. Efimova, L. M. Ostrovskaya, O. S. Serebryannikova and M. I. Tsypin, *Sov. Phy. Semicond.*, 1971, **4**, 1122–1125.
62 J. D. Eshelby, *Acta Metall.*, 1955, **3**, 487–490.
63 O. L. Anderson and J. E. Nafe, *J. Geophys. Res.*, 1965, **70**, 3951–3963.
64 D. L. Anderson and O. L. Anderson, *J. Geophys. Res.*, 1970, **75**, 3494–3500.
65 L. Makowski and M. Glicksman, *J. Phys. Chem. Solids*, 1973, **34**, 487–492.
66 F. Herman, M. Glicksman and R. H. Parmenter, in *Progress in semiconductors*, ed. A. F. Gibson, R. E. Burgess and P. Aigrain, John Wiley&Sons, INC, New York, 1957, vol. 2, pp. 3–33.
67 L. Nordheim, *Ann. Phys.*, 1931, **9**, 607–640.
68 J. W. Harrison and J. R. Hauser, *Phys. Rev. B: Condens. Matter Mater. Phys.*, 1976, **13**, 5347–5350.
69 J. J. Tietjen and L. R. Weisberg, *Appl. Phys. Lett.*, 1965, **7**, 261–263.
70 C. Herring and E. Vogt, *Phys. Rev.*, 1956, **101**, 944.
71 J. R. Hauser, M. A. Littlejohn and T. H. Glisson, *Appl. Phys. Lett.*, 1976, **28**, 458–461.
72 S. R. Mehrotra, A. Paul and G. Klimeck, *Appl. Phys. Lett.*, 2011, **98**, 173503.
73 S.-H. Wei and A. Zunger, *Phys. Rev. B: Condens. Matter Mater. Phys.*, 1997, **55**, 13605–13610.
74 A. D. LaLonde, T. Ikeda and G. J. Snyder, *Rev. Sci. Instrum.*, 2011, **82**, 025104.
75 K. A. Borup, E. S. Toberer, L. D. Zoltan, G. Nakatsukasa, M. Errico, J. P. Fleurial, B. B. Iversen and G. J. Snyder, *Rev. Sci. Instrum.*, 2012, **83**, 123902.
76 S. Iwanaga, E. S. Toberer, A. Lalonde and G. J. Snyder, *Rev. Sci. Instrum.*, 2011, **82**, 063905.
77 R. Blachnik and R. Igel, *Z. Naturforsch., B: Chem. Sci.*, 1974, **B 29**, 625–629.

